IOP PUBLISHING JOURNAL OF PHYSICS A: MATHEMATICAL AND THEORETICAL

J. Phys. A: Math. Theor. 45 (2012) 395001 (10pp) doi:10.1088/1751-8113/45/39/395001

Exact solution of a model of a vesicle attached to a wall subject to mechanical deformation

A L Owczarek[1] and T Prellberg[2]

[1] Department of Mathematics and Statistics, The University of Melbourne, Parkville, Victoria 3010, Australia
[2] School of Mathematical Sciences, Queen Mary University of London, Mile End Road, London E1 4NS, UK

E-mail: owczarek@unimelb.edu.au and t.prellberg@qmul.ac.uk

Received 14 November 2011, in final form 6 August 2012
Published 11 September 2012
Online at stacks.iop.org/JPhysA/45/395001

Abstract

Area-weighted Dyck-paths are a two-dimensional model for vesicles attached to a wall. We model the mechanical response of a vesicle to a pulling force by extending this model. We obtain an exact solution using two different approaches, leading to a q-deformation of an algebraic functional equation, and a q-deformation of a linear functional equation with a catalytic variable, respectively. While the non-deformed linear functional equation is solved by substitution of special values of the catalytic variable (the so-called kernel method), the q-deformed case is solved by iterative substitution of the catalytic variable. Our model shows a non-trivial phase transition when a pulling force is applied. As soon as the area is weighted with non-unity weight, this transition vanishes.

PACS numbers: 02.10.Ox, 05.50.+q, 05.70.Fh

(Some figures may appear in colour only in the online journal)

1. Introduction

With the growing experimental ability to probe the behaviour of a single polymer under the influence of a stretching force [13, 12], there has been an effort by theoretical work to explore models that cover the possible scenarios encountered. For example, various directed path models of a polymer with one end, or both ends, grafted to a surface and being pulled at the end or in the middle, with the addition of an attractive contact interaction with the surface, have been studied in two and three dimensions [22, 23, 6, 1, 15]. Numerical work on self-avoiding walks models has also confirmed and expanded upon the predictions of these directed models [16, 17, 20, 21]. In the continuum limit, this problem is related to the area under a Brownian curve [19].

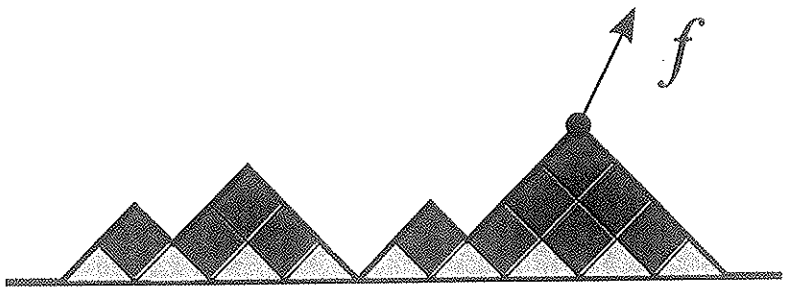

Figure 1. An area-weighted Dyck path with 18 steps and area of size 11, which is being pulled away from the surface at its right-most peak with force f. The height h of the right-most peak in this example is 4.

Another type of model, that of a lattice polygon that has been weighted by its length and area, can rather be used to model biological vesicles [18, 2–5, 9, 24]. For example, the effect of a restricted geometry such as a slit has recently been analysed [25]. Here, it is also natural to consider the effect of a pulling force of the surface of the vesicle.

Pulling membrane-anchored microspheres using optical traps is a technique commonly used in experimental settings [28]. When preparing the sample, microspheres can bind anywhere on the membrane, and due to small anisotropies in the experimental setup perfect vertical pulling is difficult to achieve.

Hence, we study a simple directed model of a two-dimensional vesicle that is being pulled away from a wall. The anisotropy is modelled by a pulling force with a small horizontal component, which leads to the force acting on the right-most peak of the vesicle. Only the vertical component of the force contributes to the configurational energy of the vesicle.

The model is of interest physically as well as mathematically. It illustrates the solution of functional equations with catalytic variables under a q-deformation, when the solution gets expressed in terms of q-series rather than in terms of algebraic functions.

2. The model

Dyck paths are directed walks on $\mathbb{Z}^2$ starting at $(0, 0)$ and ending on the line $y = 0$, which have no vertices with negative y-coordinates, and which have steps in the $(1, 1)$ (up-step) and $(1, -1)$ (down-step) directions [29]. Given a Dyck path π, we define the length $n(\pi)$ to be half the number of its steps, and the area $m(\pi)$ to be the sum of the starting heights of all up-steps in the path. This is sometimes also called the rank function of a Dyck path [8, 27], and is equivalent to the number of diamond plaquettes under the Dyck path. We further define the height $h(\pi)$ of the right-most peak as the length of the final descent of the Dyck path, i.e. the maximal number of the last consecutive down-steps. An example of a Dyck path is given in figure 1.

Let $\mathcal{G}$ be the set of Dyck paths, and define the generating function

$$G(t, q, \lambda) = \sum_{\pi \in \mathcal{G}} t^{n(\pi)} q^{m(\pi)} \lambda^{h(\pi)}. \tag{2.1}$$

The generating function for area-weighted Dyck paths [10, 7] has previously been studied. Dyck paths weighted by height of the right-most peak are related to Ballot paths, which have been previously studied as a model of pulled polymers [22]. Here we extend these works by combining and extending these models.

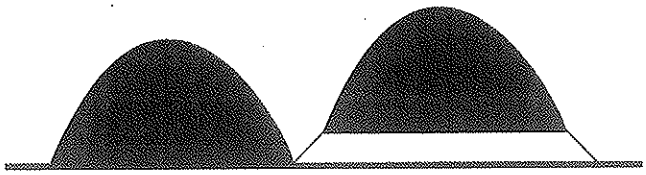

Figure 2. A schematic decomposition leading to equation (3.1). A non-zero Dyck path decomposes uniquely into a Dyck path, followed by another Dyck path which is bracketed by up and down steps.

The key to obtaining a solution of this model is a combinatorial construction of Dyck paths which leads to a functional equation for the generating function G. We shall present two different constructions leading to two structurally different functional equations.

3. q-deformed algebraic functional equation

To obtain the first functional equation, we decompose Dyck paths by considering the right-most up-step starting at height zero. This leads to a decomposition of a Dyck path in terms of two smaller Dyck paths. More precisely, except for the zero-step path, this decomposes a Dyck path uniquely into a Dyck path, followed by another Dyck path which is bracketed by up and down steps, as indicated in figure 2.

This naturally leads to a functional equation which is quadratic in the generating functions,

$$G(t, q, \lambda) = 1 + \lambda t G(t, q, 1) G(qt, q, \lambda). \tag{3.1}$$

Note that in the product $\lambda t G(t, q, 1) G(qt, q, \lambda)$ the left Dyck path no longer contributes to the height of the right-most peak, leading to the factor $G(t, q, 1)$, and the bracketing of the right Dyck path by up and down steps increases the area proportional to the length of the path, as well as increases height and length by 1, leading to the factor $\lambda t G(qt, q, \lambda)$.

3.1. The case $q = 1$

The functional equation (3.1) reads now

$$G(t, 1, \lambda) = 1 + \lambda t G(t, 1, 1) G(t, 1, \lambda), \tag{3.2}$$

which after substitution of $\lambda = 1$ can be readily solved to give

$$G(t, 1, 1) = \frac{1 - \sqrt{1 - 4t}}{2t} = \frac{2}{1 + \sqrt{1 - 4t}}, \tag{3.3}$$

which is the well-known generating function for Catalan numbers. Substitution of this result back into equation (3.2) gives

$$G(t, 1, \lambda) = \frac{2}{2 - \lambda + \lambda\sqrt{1 - 4t}}. \tag{3.4}$$

For comparison with the result in equation (3.11), note that a series expansion in λ gives

$$G(t, 1, \lambda) = \sum_{l=0}^{\infty} \lambda^l t^l G(t, 1, 1)^l. \tag{3.5}$$

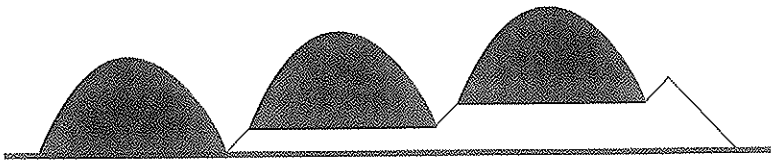

Figure 3. The term $l = 3$ in the sum of (3.11) corresponds to the concatenation of three Dyck paths separated by single up-steps, followed by a hook formed of one up-step and three down-steps.

3.2. The case $q \neq 1$

Substituting $\lambda = 1$ into the functional equation (3.1) gives

$$G(t, q, 1) = 1 + tG(t, q, 1)G(qt, q, 1). \tag{3.6}$$

The Ansatz

$$G(t, q, 1) = \frac{H(qt, q)}{H(t, q)} \tag{3.7}$$

gives a linear functional equation for $H(t, q)$,

$$H(qt, q) = H(t, q) + tH(q^2t, q). \tag{3.8}$$

Inserting $H(t, q) = \sum_{n=0}^{\infty} c_n(q)t^n$ into (3.8) gives a recurrence $q^n c_n(q) = c_n(q) + q^{2(n-1)}c_{n-1}(q)$ for the coefficients, which can be readily solved by iteration. Specializing to $c_0(q) = 1$, we find

$$H(t, q) = \sum_{k=0}^{\infty} \frac{(-t)^k q^{k(k-1)}}{(q; q)_k}, \tag{3.9}$$

where we have used the q-product notation

$$(t; q)_k = \prod_{j=0}^{k-1}(1 - tq^j). \tag{3.10}$$

Here $H(t, q) = {}_0\phi_1(-; 0; q, -t)$ is a basic hypergeometric series [11] also referred to as the q-Airy function [14].

Once $G(t, q, 1)$ is known and substituted back into equation (3.1), we can solve for $G(t, q, \lambda)$ by iteration and obtain

$$G(t, q, \lambda) = \sum_{l=0}^{\infty} \lambda^l t^l q^{\binom{l}{2}} \frac{H(q^l t, q)}{H(t, q)}. \tag{3.11}$$

This iteration makes sense in a ring of formal power series. Alternatively, one can argue that the iteration converges for $|q| < 1$.

We note that this solution also admits a direct combinatorial interpretation. The lth term in the sum of (3.11) corresponds to the concatenation of l Dyck paths separated by single up-steps, followed by a final hook formed by one up-step and l down-steps. The generating function for a Dyck path starting at height l is given by $G(q^l t, q, 1)$, and the final descent of length l increases the area by $\binom{l}{2}$, leading to an overall weight of

$$G(t, q, 1)tG(qt, q, 1)t \cdot \ldots \cdot G(q^l t, q, 1)t\lambda^l q^{\binom{l}{2}} = \lambda^l t^l q^{\binom{l}{2}} \frac{H(q^l t, q)}{H(t, q)}. \tag{3.12}$$

Figure 3 indicates this for the case $l = 3$.

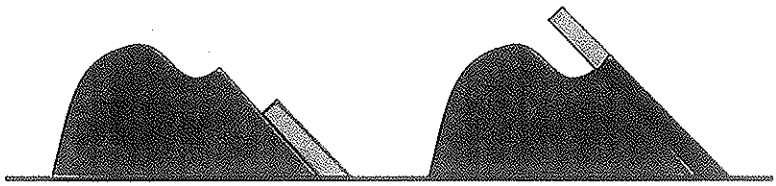

Figure 4. A schematic construction leading to equation (4.1). Inserting an up-step followed immediately by a down-step in the right-most descent creates a new Dyck path with a new hook (left). When adding hooks of all possible lengths, one needs to correct for overhangs produced by hooks that are too long (right).

Finally, we note that the limit $q \to 1$ can be obtained as follows. As

$$G(t, 1, 1) = \lim_{q\to 1} G(t, q, 1) = \lim_{q\to 1} \frac{H(qt, q)}{H(t, q)}, \tag{3.13}$$

we deduce that for fixed value of k,

$$G(t, 1, 1) = \lim_{q\to 1} \frac{H(q^{k+1}t, q)}{H(q^k t, q)} \tag{3.14}$$

and thus

$$\lim_{q\to 1} \frac{H(q^l t, q)}{H(q, t)} = G(t, 1, 1)^l. \tag{3.15}$$

Therefore equation (3.11) reduces to the result in equation (3.5) as $q \to 1$.

4. q-deformed linear functional equation

To obtain the second functional equation, we consider how Dyck path configurations get changed by the insertion of a small pattern.

The right-most descent, together with the preceding up-step forms a *hook*. Inserting an up-step followed immediately by a down-step in the right-most descent creates a new Dyck path with a new hook. If the descent has length h, there are $h + 1$ possibilities of insertion.

The consequence of this insertion is the addition of a column to the Dyck path as indicated on the left-hand-side of figure 4.

The functional equation corresponding to this construction is given by

$$G(t, q, \lambda) = 1 + \frac{\lambda t}{1 - q\lambda} G(t, q, 1) - \frac{q\lambda^2 t}{1 - q\lambda} G(t, q, q\lambda). \tag{4.1}$$

The term $\frac{\lambda t}{1-q\lambda} G(t, q, 1)$ corresponds to the addition of a column of arbitrary height to the Dyck path. The ensuing overcounting is compensated for by subtraction of the term $\frac{q\lambda^2 t}{1-q\lambda} G(t, q, q\lambda)$, which corresponds to the removal of the columns that produce invalid configurations, as indicated on the right-hand-side of figure 4.

Alternatively, the terms on the right-hand side of (4.1) can be understood by considering

$$G(t, q, \lambda) = \sum_{h=0}^{\infty} \lambda^h G_h(t, q), \tag{4.2}$$

where $G_h(t, q)$ are partial generating functions for fixed height h. The only Dyck path with a hook of height $h = 0$ is a zero-step path. A Dyck path with a hook of height $h \geqslant 1$ can

only have been constructed from a Dyck path with a hook of height at least $h-1$. By the construction, its area increases by an amount $h-1$, and we thus find that for $h \geqslant 1$

$$G_h(t,q) = q^{h-1} \sum_{k=h-1}^{\infty} G_k(t,q). \tag{4.3}$$

Summing over the partial generating functions leads to the functional equation (4.1).

4.1. The case $q = 1$

The functional equation (4.1) now reads

$$G(t,1,\lambda) = 1 + \frac{\lambda t}{1-\lambda} G(t,1,1) - \frac{\lambda^2 t}{1-\lambda} G(t,1,\lambda). \tag{4.4}$$

Here, substitution of $\lambda = 1$ is no longer useful, and one solves the functional equation using the kernel method [26]. Writing equation (4.1) as

$$K(t,\lambda) G(t,1,\lambda) = 1 + \frac{\lambda t}{1-\lambda} G(t,1,1), \tag{4.5}$$

where the kernel $K(t,\lambda)$ is given as

$$K(t,\lambda) = 1 + \frac{\lambda^2 t}{1-\lambda}, \tag{4.6}$$

we observe that the left-hand side of equation (4.5) vanishes if $\lambda = \lambda_0$ is chosen such that $K(t,\lambda_0)$ vanishes (provided $G(t,1,\lambda_0)$ does not diverge). This then implies that

$$G(t,1,1) = \frac{\lambda_0 - 1}{\lambda_0 t}, \tag{4.7}$$

and substituting this result back into equation (4.5) leads to an expression for $G(t,1,\lambda)$. The appropriate root of the kernel is given by

$$\lambda_0 = \frac{1-\sqrt{1-4t}}{2t}. \tag{4.8}$$

Using this value, we recover the expressions (3.3) for $G(t,1,1)$ and (3.4) for $G(t,1,\lambda)$ given above.

4.2. The case $q \neq 1$

If $q \neq 1$, we can solve the functional equation (4.1) by iterative substitution. Substituting λq^k for λ in (4.1), we find

$$G(t,q,q^k\lambda) = 1 + \frac{q^k \lambda t}{1-q^{k+1}\lambda} G(t,q,1) - \frac{q^{2k+1}\lambda^2 t}{1-q^{k+1}\lambda} G(t,q,q^{k+1}\lambda). \tag{4.9}$$

We can therefore express $G(t,q,q^k\lambda)$ in terms of $G(t,q,q^{k+1}\lambda)$ and use this to iterate. As a result, we find

$$G(t,q,\lambda) = \sum_{k=0}^{\infty} \frac{(-\lambda^2 t)^k q^{k^2}}{(q\lambda;q)_k} \left(1 + \frac{q^k \lambda t}{1-q^{k+1}\lambda} G(t,q,1)\right). \tag{4.10}$$

Defining

$$I(t,q,y) = \sum_{k=0}^{\infty} \frac{(-t)^k q^{k(k-1)}}{(y;q)_k}, \tag{4.11}$$

this simplifies to

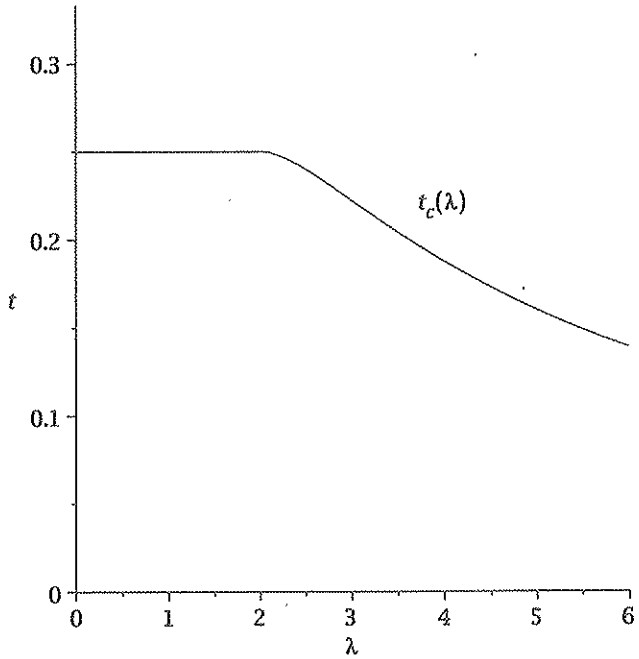

Figure 5. A plot of the radius of convergence $t_c(\lambda) \equiv t_c(\lambda, 1)$ in the polymer length variable t of the generating function when $q = 1$ as a function of the force variable λ. Note that there is a change of behaviour at $\lambda = 2$ with constant $t_c(\lambda) = 1/4$ for $\lambda \leqslant 2$.

$$G(t, q, \lambda) = I(q\lambda^2 t, q, q\lambda) - \frac{1}{\lambda}[I(\lambda^2 t, q, q\lambda) - 1]G(t, q, 1). \tag{4.12}$$

Note that $I(t, q, y) = {}_1\phi_2(q; 0, y; q, -t)$ is also expressible as a basic hypergeometric function. Moreover, it a deformation of $H(t, q)$, in that $I(t, q, q) = H(t, q)$.

Substituting $\lambda = 1$ in equation (4.12) gives now immediately

$$G(t, q, 1) = \frac{H(qt, q)}{H(t, q)}, \tag{4.13}$$

a result already obtained from the q-algebraic functional equation (3.6) above. Substituting this result back into equation (4.12) leads to the main result of this section, namely

$$G(t, q, \lambda) = I(q\lambda^2 t, q, q\lambda) - \frac{1}{\lambda}[I(\lambda^2 t, q, q\lambda) - 1]\frac{H(qt, q)}{H(t, q)}. \tag{4.14}$$

Note the rather different structure of the equivalent solutions (3.11) and (4.14). The former is in terms of an infinite sum, which however readily allows for extraction of the partial generating function for fixed height h. The latter is more compact as it is written in terms of a finite number of special functions. We note that the equivalence of both solutions implies the identity

$$\sum_{l=0}^{\infty} \lambda^l t^l q^{\binom{l}{2}} H(q^l t, q) = I(q\lambda^2 t, q, q\lambda)H(t, q) - \frac{1}{\lambda}\big[I(\lambda^2 t, q, q\lambda) - 1\big]H(qt, q). \tag{4.15}$$

5. Analysis of behaviour

Let us begin by considering the case of $q = 1$, that is no extra area weighting or, equivalently, osmotic pressure. The first important point to make is that previous models of pulling on the

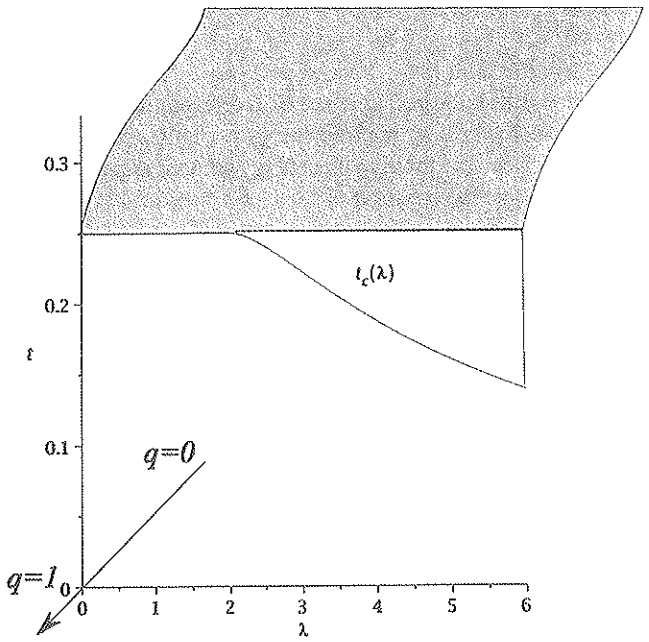

Figure 6. A plot of the radius of convergence $t_c(\lambda, q)$ in the polymer length variable t of the generating function for general q as a function of the force variable λ. Note that $t_c(\lambda, q)$ is independent of q for $q < 1$ and hence that there is a jump of $t_c(\lambda, q)$ as q approaches one from below.

end of a polymer without any other interaction with a surface give the result that as soon as a force is applied the end of the polymer changes its scaling behaviour from random-walk scaling

$$\langle h \rangle \sim n^{1/2} \tag{5.1}$$

for $f = 0$ ($\lambda = 1$) to ballistic scaling

$$\langle h \rangle \sim n \tag{5.2}$$

for $f > 0$ ($\lambda > 1$). This is reflected in the fact that the radius of convergence of the associated generating function is constant for $\lambda \leqslant 1$ and decreases continuously for $\lambda > 1$. As a model of pulling on a vesicle attached to a surface, our model has the feature that the pulling occurs on the final 'peak', the location of which along the surface can change with the pulling itself. As such, there is a non-trivial critical point as a function of λ in our model, with a critical value

$$\lambda = \lambda_c \equiv 2. \tag{5.3}$$

A plot of the radius of convergence of the generating function (3.4) is shown in figure 5.

Note that the reduced free energy $\kappa(\lambda, q)$ of the surface is simply related to the radius of convergence $t_c(\lambda, q)$ in the usual way via

$$\kappa(\lambda, q) = -\log t_c(\lambda, q). \tag{5.4}$$

For $q < 1$ the generating function (3.11) can be seen to be convergent except where $H(t, q) = 0$. Crucially this is independent of λ! This implies that for $q < 1$ there is no phase transition as a function of λ, since $\kappa(\lambda, q)$ is independent of λ for $q < 1$. Physically this means

that the osmotic pressure always dominates the pulling force for $q < 1$: $\langle h \rangle$ will be bounded for all λ.

Interestingly, if one considers the limit $q \to 1$ for $\lambda > 2$ one is left with the problem that the free energy 'jumps' at $q = 1$ as indicated in figure 6. The resolution of this apparent problem is that for $q > 1$ one needs to consider the free energy per unit area rather than the free energy per unit length of the surface. The limiting free energy per unit area is a continuous function of q and λ for all λ, being equal to zero for $q \leqslant 1$.

6. Conclusion

We have provided the exact solution of a simple model of a vesicle attached to a surface subject to a pulling force on the vesicle. We have used two methods of solution which illuminate the generalization of the well-known 'kernel' method for the solution of linear functional equations using a 'catalytic' variable and result in a non-trivial identity. The solution is expressed in terms of well-studied q-series and can be analysed simply. Our model has a non-trivial phase transition when no osmotic pressure is applied.

Acknowledgments

Financial support from the Australian Research Council via its support for the Centre of Excellence for Mathematics and Statistics of Complex Systems is gratefully acknowledged by the authors. ALO thanks the School of Mathematical Sciences, Queen Mary University of London for hospitality.

References

[1] Alvarez J and Whittington S G 2009 Force-extension relations for adsorbing polymers subject to a force *J. Stat. Mech.* P04016

[2] Brak R and Guttmann A J 1990 Exact solution of a staircase and row-convex polygon perimeter and area generating function *J. Phys. A: Math. Gen.* **23** 4581

[3] Brak R, Owczarek A L and Prellberg T 1994 Exact scaling behaviour of partially convex vesicles *J. Stat. Phys.* **76** 1101

[4] Brak R, Essam J M and Owczarek A L 1998 New results for directed vesicles and chains near an attractive wall *J. Stat. Phys.* **93** 155

[5] Brak R, Owczarek A L, Rechnitzer A and Whittington S 2005 A directed walk model of a long chain polymer in a slit with attractive walls *J. Phys. A: Math. Gen.* **38** 4309

[6] Brak R, Dyke P, Lee J, Owczarek A L, Prellberg T, Rechnitzer A and Whittington S 2009 A self-interacting partially directed walks subject to a force *J. Phys. A: Math. Theor.* **42** 085001

[7] Duchon P 2000 On the enumeration and generation of generalized Dyck words *Discrete Math.* **225** 121

[8] Ferrari L and Pinzani R 2005 Lattices of lattices paths *J. Stat. Plan. Inference* **135** 7792

[9] Fisher M E, Guttmann A J and Whittington S 1991 *J. Phys. A: Math. Gen.* **24** 3095

[10] Flajolet P 1980 Combinatorial aspects of continued fractions *Discrete Math.* **41** 125

[11] Gasper G and Rahman M 2004 *Basic Hypergeometric Series (Encyclopedia of Mathematics and Its Applications* vol 96*)* (Cambridge: Cambridge University Press)

[12] Hauchke H, Miles M J and Koutsos V 2004 Conformation of a single polyacrylamide molecule adsorbed onto a mica surface studied with atomic force microscopy *Macromolecules* **37** 3799

[13] Haupt B J, Ennis J and Sevick E M 1999 The detachment of a polymer chain from a weakly adsorbing surface using an AFM tip *Langmuir* **15** 3886

[14] Ismail M E H 2005 Asymptotics of q-orthogonal polynomials and a q-Airy function *Int. Math. Res. Not.* **2005** 1063

[15] Janse van Rensburg E J 2010 Pulled directed lattice paths *J. Phys. A: Math. Theor.* **43** 215001

[16] Krawczyk J, Prellberg T, Owczarek A L and Rechnitzer A 2004 Stretching of a chain polymer adsorbed at a surface *J. Stat. Mech.* P10004

[17] Krawczyk J, Owczarek A L, Prellberg T and Rechnitzer A 2005 Pulling absorbing and collapsing polymers from a surface *J. Stat. Mech.* P05008
[18] Leibler S, Singh R R P and Fisher M E 1987 Thermodynamic behavior of two-dimensional vesicles *Phys. Rev. Lett.* **59** 1989
[19] Majumdar S N and Comtet A 2005 Airy distribution function: from the area under a Brownian excursion to the maximal height of fluctuating interfaces *J. Stat. Phys.* **119** 777
[20] Mishra P K, Kumar S and Singh Y 2005 Force-induced desorption of a linear polymer chain adsorbed on an attractive surface *Europhys. Lett.* **69** 102
[21] Orlandini E and Tesi M C 2009 Modelling the adsorption of a polymer subject to an elongational force by directed walk models *J. Math. Chem.* **45** 72
[22] Orlandini E and Whittington S G 2004 Pulling a polymer at an interface: directed walk models *J. Phys. A: Math. Gen.* **37** 5305
[23] Orlandini E, Tesi M C and Whittington S G 2004 Adsorption of a directed polymer subject to an elongational force *J. Phys. A: Math. Gen.* **37** 1535
[24] Owczarek A L and Prellberg T 1993 Exact solution of the discrete (1+1)-dimensional SOS model with field and surface interactions *J. Stat. Phys.* **70** 1175
[25] Owczarek A L and Prellberg T 2010 A simple model of a vesicle drop in a confined geometry *J. Stat. Mech.* P08015
[26] Prodinger H 2004 The kernel method: a collection of examples *Sém. Lothar. Comb.* **50** B50f
[27] Sapounakis A, Tasoulas I and Tsikouras P 2006 On the dominance partial ordering of Dyck paths *J. Integer Sequences* **9** 06.2.5
[28] Settles E I, Loftus A F, McKeown A N and Parthasarathy R 2010 The vesicle trafficking protein Sar1 lowers lipid membrane rigidity *Biophys. J.* **99** 1539
[29] Stanley R P 1999 *Enumerative Combinatorics* vol 2 *(Cambridge Studies in Advanced Mathematics* vol 62) (Cambridge: Cambridge University Press)